SUPPORTING INFORMATION

Chemistry of Aqueous Silica Nanoparticle Surfaces and the Mechanism of Selective Peptide Adsorption

Siddharth V. Patwardhan, Fateme S. Emami, Rajiv J. Berry, Sharon E. Jones, Rajesh R. Naik, Olivier Deschaume, Hendrik Heinz, and Carole C. Perry

S1. Experimental Procedures

S1.1. Reagents

Tetramethyl orthosilicate, ≥99% (TMOS), dipotassium silicon triscatecholate ($K_2[Si(C_6H_4O_2)_3].2H_2O$, 97% (Si-Cat), tetraethyl orthosilicate, 98% (TEOS), piperazine, N,N-diisopropylethylamine (DIPEA), trifluoroacetic acid (TFA), thioanisole (TIS), 3,6-dioxa-1,8-octanedithiol (DODT), fluorescamine 98%, sodium chloride, monosodium phosphate, disodium phosphate, Trizma base, anhydrous sodium sulfite 97%, standard 1M HCl and 1M NaOH were purchased from Sigma-Aldrich. Ammonium molybdate, hydrochloric acid 37%, sodium hydroxide (pellets, ≥97%), sulfuric acid 98%, N,N-dimethylformamide (DMF), dichloromethane (DCM), N-methyl-2-pyrrolidinone (NMP), and diethyl ether were purchased from Fisher Scientific. Oxalic acid 99% and p-methylamino phenol sulfate 99% were purchased from Acros Chemicals and standard stabilised silicate solution (1000 ppm as SiO_2) was purchased from BDH. HBTU, (O-nenzotriazole-N,N,N',N'-tetramethyl-uronium-hexafluoro-phosphate) and all Fmoc-protected amino acids required for peptide synthesis were purchased from CEM Corporation while the preloaded Wang resins were obtained from Merck Chemicals. CBQCA Protein Quantitation Kit containing ATTO-TAG™ CBQCA reagent 3-(4-

carboxybenzoyl)quinoline-2-carboxaldehyde, dimethylsulfoxide (DMSO), potassium cyanide and bovine serum albumin was obtained from Molecular Probes. All chemicals except Si-Cat were used without further treatment. Si-Cat was dissolved in methanol and recrystallised; its purity was checked by ^{1}H-NMR (single peak at 6.63 ppm for complexed protons). Distilled deionised water (ddH_2O) having conductivity less than 1μScm^{-1} was used for all preparations when required.

S1.2. Measurement of Peptide Adsorption

Three independent peptide quantification methods were compared: (1) a direct UV absorbance measurement, (2) the 3-(4-carboxybenzoyl)quinoline-2-carboxaldehyde (CBQCA) assay[S1] and (3) a fluorescamine assay.[58] The latter method was used in this investigation since it was found to be the most reliable, rapid, safe, and suitable for all peptides under consideration (**Figure S1**). The peptide concentrations in the supernatant were calculated using calibration data obtained from standards of the same peptide solutions used in the binding studies. The peptide concentration in the sample aliquots was always maintained in the linear range of the calibration. Fluorescence measurements using fluorescamine performed in the absence of peptide but in the presence of silica particles revealed that silica does not interfere with the measurements.

The gravimetric amount of peptide adsorbed in mg/mL was converted into number of molecules per surface area as follows. (1) The gravimetric concentration of silica of 1 mg/mL, which was constant throughout all studies, was converted into volume of silica particles per volume of solvent using the experimentally determined density of the respective silica particles. (2) The total number of silica particles per unit volume of solvent was then calculated using the known volume of each particle for each particle size batch. The total surface area of all silica

particles was calculated from the number of particles per unit volume. (3) The measured gravimetric concentration of adsorbed peptide in mg/mL was converted into a molar concentration of adsorbed peptide in mmol/mL and the molar amount of peptide adsorbed. The relation of the molar amount of adsorbed peptide to the total surface area of all silica particles from (2) yielded the number of peptide molecules adsorbed per unit area of silica particles.

All experiments were performed after one hour incubation time. It was found that upon centrifugation and washing of the silica particles, negligible (or in some cases even undetectable) quantities of silica-bound peptides were desorbed. This suggests that the amount of loosely bound peptide was negligible and washing of centrifuged particles for the removal of loosely bound peptides was not essential.

S1.3. ATR-FTIR and XPS of Adsorbed Peptides

Attenuated Total Reflection Fourier Transform Infrared Spectroscopy (ATR-FTIR; either PerkinElmer Spectrum 100 Series or Thermo Nicolet Magna IR-750 spectrophotometer) was used for qualitative detection of peptide adsorption on silica particles. After the incubation of the silica-peptide samples as described above, the samples were centrifuged, washed and lyophilized. These sample powders were placed on a diamond crystal of the ATR-FTIR and scanned from 4000-380 cm^{-1} at a resolution of 1 cm^{-1}.

XPS measurements were performed using an M-PROBE Surface Science XPS spectrometer utilizing charge neutralization. Samples were prepared by dropcasting 10 μl of an aqueous suspension onto an Al sample holder and air dried. Spectra were collected from 0-1000 eV at 1 eV steps at a spot size of 800 μm and averaged over 15 scans for standard resolution. For high resolution scans, spectra were collected at 0.065 eV steps and averaged over 50 scans.

S1.4. Silica Condensation, Precipitation, and Characterization

The concentration of silicic acid during silica condensation was determined by the absorbance of the blue silicomolybdate complex at 810 nm using a Unicam UV2 UV-VIS spectrometer. Calibration of this method using a standard silicate solution showed a linear relationship between concentration and absorbance over the whole concentration range used.[6]

TMOS was used to assess the amount of silica that could be precipitated in the presence of a given peptide. Typically, to a 100 mM pre-hydrolysed solution of TMOS, the desired amount of peptide was added (0-1 mg mL^{-1}), mixed thoroughly and left to react for 15 mins; after which the solutions were centrifuged and the supernatant discarded. The precipitate was then dissolved in 2 M NaOH at 80^{o}C for 1 h before taking an aliquot for silica quantification as described above using the molybdenum blue method.

Characterization of centrifuged and lyophilized samples obtained from silica precipitation experiments using SiCat was performed using Scanning Electron Microscopy (SEM; Philips FEI XL30 FEG-ESEM). The lyophilized samples were placed onto double sided sticky carbon tape placed on aluminium sample holders. Prior to SEM analysis, the samples were sputter coated with gold under argon plasma to minimize sample charging.

S1.5. Reliability of Measurements

Error analysis was performed on all experimental data by calculation of the statistical significance using the Student *t*-test. All error bars indicate a high confidence interval of 95% corresponding to α=0.05.

S2. Computational Procedures

S2.1. Models. We employed models of even silica surfaces of Q^3 environment, i.e., a chemical environment of $(Si–O–)_3Si(–OH)$ or $(Si–O–)_3Si(–O^- \cdots Na^+)$ for superficial Si atoms with one silanol or sodium siloxide group, as well as even silica surfaces of Q^2 environment, i.e., a chemical environment of $(Si–O–)_2Si(–OH)_2$ or $(Si–O–)_2Si(–OH)(–O^- \cdots Na^+)$ for superficial Si atoms with two silanol or sodium siloxide groups. Q^3 environments are more common on amorphous silica surfaces than Q^4, Q^2 and other environments. The model surfaces of Q^3 silica were prepared from the [1 0 -1] cleavage plane of α-cristobalite and hydration to form silanol groups, and match the typical area density of 4.7 silanol groups per nm^2 surface area reported in experimental studies.[32,33] This even Q^3 surface contains isolated and vicinal silanol groups, and models with 0%, 9%, 18%, and 50% deprotonation of silanol groups to sodium siloxide were prepared to explore the typical experimental range of 4% to 21% ionization according to laboratory measurements at pH=7.5 and at lower pH values.[25-32] The pre-set differences in ionization in the models represent different ratios between isolated and vicinal silanol groups as well as different ionic strength, which are the main causes of variation in surface acidity at constant pH in experiment. To the best of our knowledge, the degree of surface ionization has been entirely neglected in earlier computational studies on silica.[35-37,40,42,43,45-47] The model of a hypothetical even Q^2 silica surface was derived from the [1 0 0] cleavage plane of α-quartz with a density of 9.4 silanol groups per nm^2 surface area and we assumed 50% ionization of the geminal silanol groups to sodium siloxide.

We note that the surface topology of amorphous silica nanoparticles varies and includes a variety of environments, defects, and cavitations. On the comparatively small length scale of the

peptides (2-3 nm) and of the models in the simulation (3-5 nm), however, the nanoparticle surfaces are in first order approximation even and were thus represented as even surfaces.

Models of the peptides were prepared using the Hyperchem and Materials Studio graphical interfaces.[59] The protonation state of the peptides was adjusted to pH=7.5 and an excess of charged residues K(+), R(+), and D(-) in the peptides was compensated by chloride and sodium counter ions. For each peptide, about ten independent secondary start structures were generated (extended, helical, random).

For each surface-peptide combination, four simulation boxes containing silica-peptide-water, silica-water, peptide-water, and water only were generated to analyze peptide interactions with the surface, peptide conformations in solution, and to compute the adsorption energy.[48] These model structures with 3D periodicity were composed of a silica slab of a thickness of ~2.5 nm, 1600 explicit water molecules, and one peptide molecule per simulation box of total dimensions of approximately 3×3×8 nm^3. Independent simulations with larger 3D periodic structures of approximately 5×5×10 nm^3 size, 5000 explicit water molecules, and one peptide molecule were also carried out. The exact cell dimensions were obtained in the course of NPT simulation at atmospheric pressure. Alternatively, the exact cell dimensions for each system were determined by addition of equilibrium dimensions and molecular volumes of all components derived from NPT simulations (silica surface, water, and peptide) in subsequent NVT simulations, and lead to identical results. For each set of calculations for a surface-peptide combination, a total of 10 periodic model structures with different initial conformations of the peptide were prepared on the surface and in solution to evaluate conformation convergence in the course of independent molecular dynamics simulations. The corresponding peptide concentration in the simulation boxes was between 35 mM and 11 mM while the effective peptide

concentration was <1 mM and <1 mg/L in all cases due to isolation of one peptide molecule per simulation box and weak residual interaction with periodic images.

S2.2. Force Field. In this study, we augmented the polymer consistent force field (PCFF)[S2] for silica (PCFF-SILICA) and employed these parameters for all components in the simulation (silica, peptides, and water). In the following, we describe briefly the concept of the simulation of the inorganic-organic interfaces, limitations of such approaches, and the new force field parameters including validation.

Classical simulations of inorganic-organic interfaces in all atomic detail are possible by use of the same classical Hamiltonian for organic and inorganic components and standard combination rules.[38,39,41,54] The necessary verification of atomic charges, van-der-Waals parameters, and bonded parameters in the force field has been previously described and can reduce common errors up to 500% in computed interfacial energies on mineral surfaces to better than 10% agreement with experiment by reproduction of key thermodynamic properties of the inorganic and organic phases in agreement with experiment.[39,41] Major properties for validation include densities, cohesive energies (predominantly for liquid components), surface tensions, interface tensions with water, and possibly adsorption energies of test compounds on the mineral surface, including high quality quantum-mechanical data. Then, computed interfacial structure and conformations, self-assembly mechanisms, adsorption energies, and nanomechanical properties usually correlate well with experimental data (e.g., XRD, IR, NMR, binding assays, TEM, AFM, calorimetry) and generate, within limits, predictions. Examples using this approach include interfaces of layered silicates with organic molecules[38,41,44,53] and interfaces of fcc metals with biomolecules.[14,50,52,54]

Limitations of such approaches include the difficulty to form or dissociate covalent bonds, the suitability of the energy expression and parameterization, difficulties in sampling conformations of large molecules, and limitations in time and length scales in the simulation. Additional information from quantum mechanical calculations and coarse-gain models, respectively, can resolve some difficulties. It is also important to be aware of the physical interpretation of individual force field parameters and the sensitivity of results to their values.

New force field parameters for silica were developed as an extension of the polymer consistent force field (PCFF).[S2] The energy expression for silica within the PCFF-SILICA force field involves terms for quadratic bond stretching, angle bending, Coulomb interactions, and van-der-Waals forces represented by a 9-6 Lennard-Jones potential:

$$E_{pot} = \sum_{ij\ \text{bonded}} K_{r,ij}(r_{ij} - r_{0,ij})^2 + \sum_{ijk\ \text{bonded}} K_{\theta,ijk}(\theta_{ijk} - \theta_{0,ijk})^2 + \frac{1}{4\pi\varepsilon_0\varepsilon_r} \sum_{\substack{ij\ \text{nonbonded} \\ (1,3\,\text{excl})}} \frac{q_i q_j}{r_{ij}} + \sum_{\substack{ij\ \text{nonbonded} \\ (1,3\,\text{excl})}} \varepsilon_{0,ij} \left(2\left(\frac{\sigma_{0,ij}}{\sigma_{ij}}\right)^9 - 3\left(\frac{\sigma_{0,ij}}{\sigma_{ij}}\right)^6 \right). \quad \text{(S1)}$$

The PCFF-PHYLLOSILICATE force field served as a starting point to derive the new parameters for silica.[41] The reasons for this choice are: (1) Silica is closely related to phyllosilicates and the atomic charges are well known,[39] (2) silica is less complex to parameterize than layered silicates, (3) densities, surface structures, cleavage energies, and interface tensions of layered silicates are reproduced in quantitative agreement with experiment using existing parameters,[41,44] (4) experimental data for the surface characterization of layered silicates are of higher quality than comparable data for silica surfaces due to large structural variation, dependence on hydration/dehydration equilibria and acid base equilibria.

The new parameters for silica are thus similar to those for phyllosilicates and reproduce key experimental properties without significant adjustments (Table S1).[39,41,44] The atomic

charges q_i of 1.1e for tetrahedral Si and –0.55e for bridging O have been previously derived in quantitative agreement with X-Ray deformation electron densities, dipole moments, an extended Born model, trends across the periodic table, and quantum-mechanical data.[39] These charges (±0.1e) are essential to compute reliable interfacial properties.[41] The van-der-Waals parameters σ_0 and ε_0 were chosen according to known atomic radii and polarizabilities[41] and slightly tuned to reproduce the density, surface tension, and interface tension of silica with water according to laboratory measurements.[34] The assignment of bonded parameters for bond stretching r_0, K_r and angle bending θ_0, K_θ leads to agreement with molecular geometry and IR spectra.[41] Deviations of r_0 and θ_0 from equilibrium bond lengths and angles according to the X-Ray structure are associated with additional Coulomb and van-der-Waals forces.[38] The parameters for silica reproduce the structure and experimental density of quartz of 2650 kg/m^3 within 1% deviation in NPT molecular dynamics simulation at 298 K and atmospheric pressure, and are consistent with the surface tension of silica surfaces of ~220 mJ/m^2 and the silica-water interface tension of ~100 mJ/m^2 reported by various groups on the basis of surface pressures,[34] assuming common Q^3 silica surfaces with 4.7 silanol groups per nm^2 and 18% ionization at pH ~ 7.5.[25-33] The impact of the wide range of laboratory data and surface compositions of silica on computed surface properties using the force field will be discussed in follow-on work. The models of silica surfaces along with the PCFF-SILICA force field cover the full range of dissociation of surface silanol groups, aiming at a full description of surface acidity as a function of surface morphology, ionic strength, and pH.

Table S1. Force field parameters for silica embedded in the polymer consistent force field (PCFF-SILICA) according to eq S1 employed in this study.

I. Charges (in units of *e*)		
Bulk silica	$[-O(-0.55)-]_4Si(+1.1)$	
On the surface	$O_3(-0.55)Si(+1.1)–O(-0.675)–H(+0.40)$	
	$O_3(-0.55)Si(+0.825)–O(-0.90) \cdots Na^+(+0.90)$	
II. Van-der-Waals	σ_0 (Å)	ε_0 (kcal/mol)
Si	4.20	0.08
O	3.60	0.04
H	1.098	0.013
Na	3.30	0.06
III. Bonds	r_0 (Å)	K_r (kcal/(mol·Å^2))
Si–O	1.68	300
O–H	0.945	495
IV. Angles	θ_0 (°)	K_θ (kcal/(mol·rad^2))
O–Si–O	109.5	100
Si–O–Si	149	100
Si–O–H	115	50

S2.3. Simulation Protocol. We carried out molecular dynamics (MD) simulations of the silica-peptide-water, silica-water, peptide-water, and water systems in the NPT ensemble at 298.15 K and 101.3 kPa, as well as in the NVT ensemble using additive molecular volumes of the constituents derived from NPT simulation.[48] MD simulations for each system consisted of an equilibration time of 1 ns followed by an analysis time of 4 ns to record atomic coordinates and thermodynamic data. Cumulative simulation times for all independent simulations of the same system were ~50 ns. The time step was 1 fs, the temperature was held constant by the Nose-Hoover thermostat and the pressure by the Nose-Hoover barostat. We applied a spherical cutoff for van-der-Waals interactions of 12 Å, and the summation of Coulomb interactions was performed using the PPPM method with a high accuracy of 10^{-6}. The program LAMMPS[59] was employed, as well as the program Discover[60] for initial testing. Energy minimization and short molecular dynamics simulations (MD) were also carried out for the peptides in water using the AMBER99 force field (**Figure 9a**).

S2.4. Analysis. The analysis involved the visual inspection of all trajectories to evaluate the structure of silica-water interfaces as well as the structure of the peptides in water and on the silica surfaces, including molecular conformations and binding geometries. We analyzed the density profile of water molecules and sodium ions on silica surfaces of different degree of ionization of silanol groups in the presence and in the absence of peptides using a bin size of 0.05 Å along the z coordinate (**Figures 6, S5, S6**). We visually analyzed the distance of individual residues of the peptides from the surface and present representative snapshots as well as superpositions of up to 2000 peptide snapshots in solution and on the surface to illustrate time-

averaged structures (**Figures 7, 8, 9, 10**). We computed adsorption energies (**Table 3**) on the basis of NPT and NVT calculations,[48] the relative surface affinity of individual amino acids without the influence of water molecules (**Figure 11a**), Ramachandran plots (**Figure 11b** and **S10**), and time-averaged NMR spectral shifts (**Figure S11**, **Table S3**).[61]

The adsorption energies of the peptides were slightly positive related to the chosen high degree of surface ionization of 50% as well as due to the high concentration of superficial sodium ions in the simulation box corresponding to ~1 mol/L related to the limited number of water molecules. Therefore, the relative trend in adsorption energies is more meaningful than the absolute values, and test simulations indicate that adsorption energies shift towards negative values for lower degree of ionization of the silica surfaces and higher dilution. Free energies are similar to the adsorption energies due to only modest conformational restrictions of the peptide upon adsorption and concomitant release of surface-bound water molecules (leading to adsorption entropy near zero).

Changes in secondary structure upon adsorption were analyzed by changes in computed NMR chemical shifts upon adsorption of the peptide from solution onto the surface (**Figure S11, Table S3**). The computational method[61] takes J-coupling into account and excludes NOEs so that conformational changes are recognized throughout the peptide, although weakly at the N and C terminal residues (**Table S3**). The larger the change is in chemical shift for a given atom, the greater are the conformational changes in its vicinity upon adsorption. Sufficiently accurate NMR measurements for comparison remained challenging and are not presented here.

S3. Further Details on Binding of Peptides

The chosen models of Q^3 surfaces indicate the presence of large and small grooves (**Figure 7, 10c,d**). The larger groove of 0.6 nm width provides more lateral space to accommodate cationic peptide groups such as NH_3^+ and guanidinium in N-termini, lysine, arginine, and bonded neighbor groups in comparison to the smaller groove of 3 nm width. Arginine with a bulkier side group than lysine fits less well and may, therefore, adsorb less strongly.

The chosen models of the Q^2 silica surface qualitatively represent a surface environment with twice the density of silanol and siloxide groups compared to the Q^3 surface, and therefore higher surface acidity. The computed relative binding strength of pep1 and pep4 is inverted on Q^2 surfaces relative to Q^3 surfaces (**Table 3**), in agreement with the experimentally observed preference of pep4 toward more acidic surfaces (450 nm silica particles) (**Figure 2**).

Table S2. Sequence similarity between silica binding peptides identified in this study and reported in the literature (ref. 16).

Peptide	Sequence	Similarity
Pep1	KSLSRHDHIHHH	
Pep2	YITPYAHLRGGN	
Pep4	MHRSDLMSAAVR	
Si4-1	MSPHPHPRHHHT	
Si4-10	RGRRRRLSCRLL	
7mer	LDHSLHS	

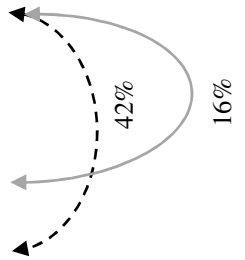

Table S3. Residues of pep1, pep1_6, and pep1_11 with the highest change (top 20%) in computed NMR chemical shifts in each category (H, C, CA, CB, N) between solution state and adsorbed state on the silica surface over a cumulative simulation period of 20 ns. Significant changes in chemical shifts indicate conformational changes upon adsorption.

Peptide	Residues with most significant changes in chemical shifts upon adsorption
Pep1	Leu3 (H, CA), Ser4 (CA), Arg5 (C, CA, CB), His6 (H, N), His8 (CB), Ile9 (N, CB, CA) , His10 (N), His11 (N)
Pep1_6	Ser2 (N), Leu3 (H), Ser4 (N), Arg5 (N), Asp7 (C, CB), Ile9 (H), His11 (H, CA), His12 (C)
Pep1_11	Ser2 (CB), Leu3 (H, C), Arg5 (N), His6 (N), Asp7 (H, C), His8 (H, N, CB), Ile9 (H, CB), Ala11 (H, N)

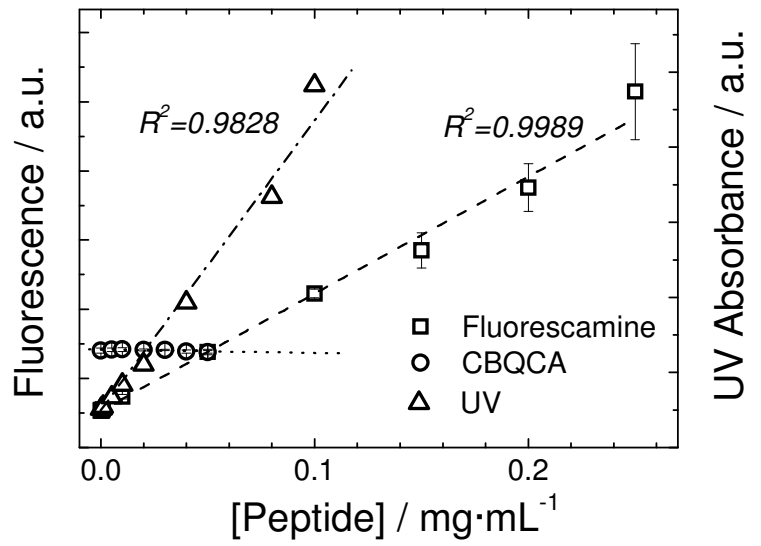

Figure S1. Comparison of assays used to quantify peptide concentrations.

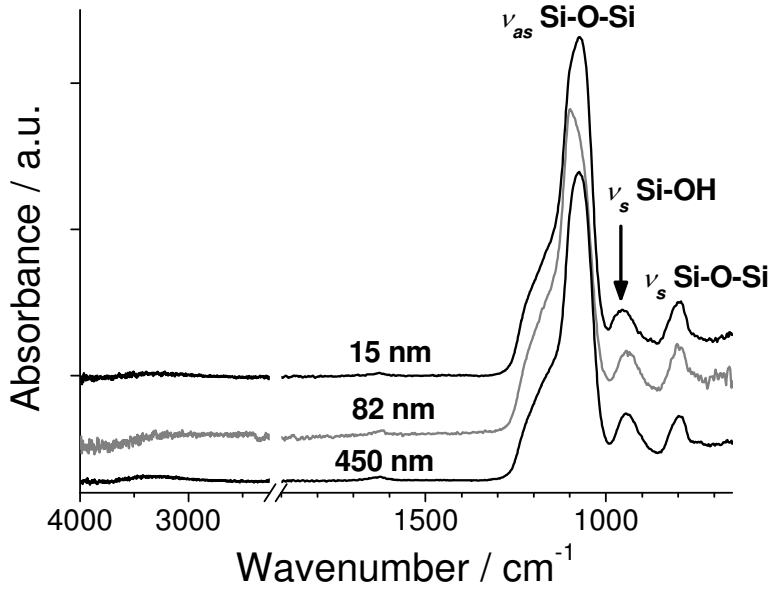

Figure S2. ATR-FTIR spectra of the three silica samples used in the biopanning experiments. Asymmetric and symmetric stretching of Si-O-Si bonds occurs at ~1070 cm^{-1} and 800 cm^{-1} respectively and Si-OH symmetric

stretching at 950 cm^{-1}. The relative intensities of the υ_s vibration Si-O-Si at ~800 cm^{-1} and of the υ_s vibration Si-OH at ~950 cm^{-1} for samples were found to be similar.

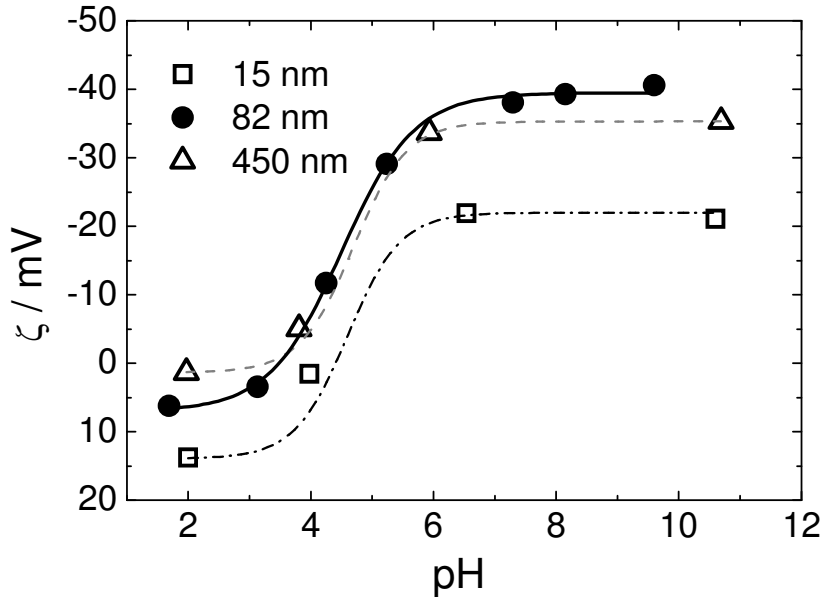

Figure S3. Zeta-potential titration of silica samples.

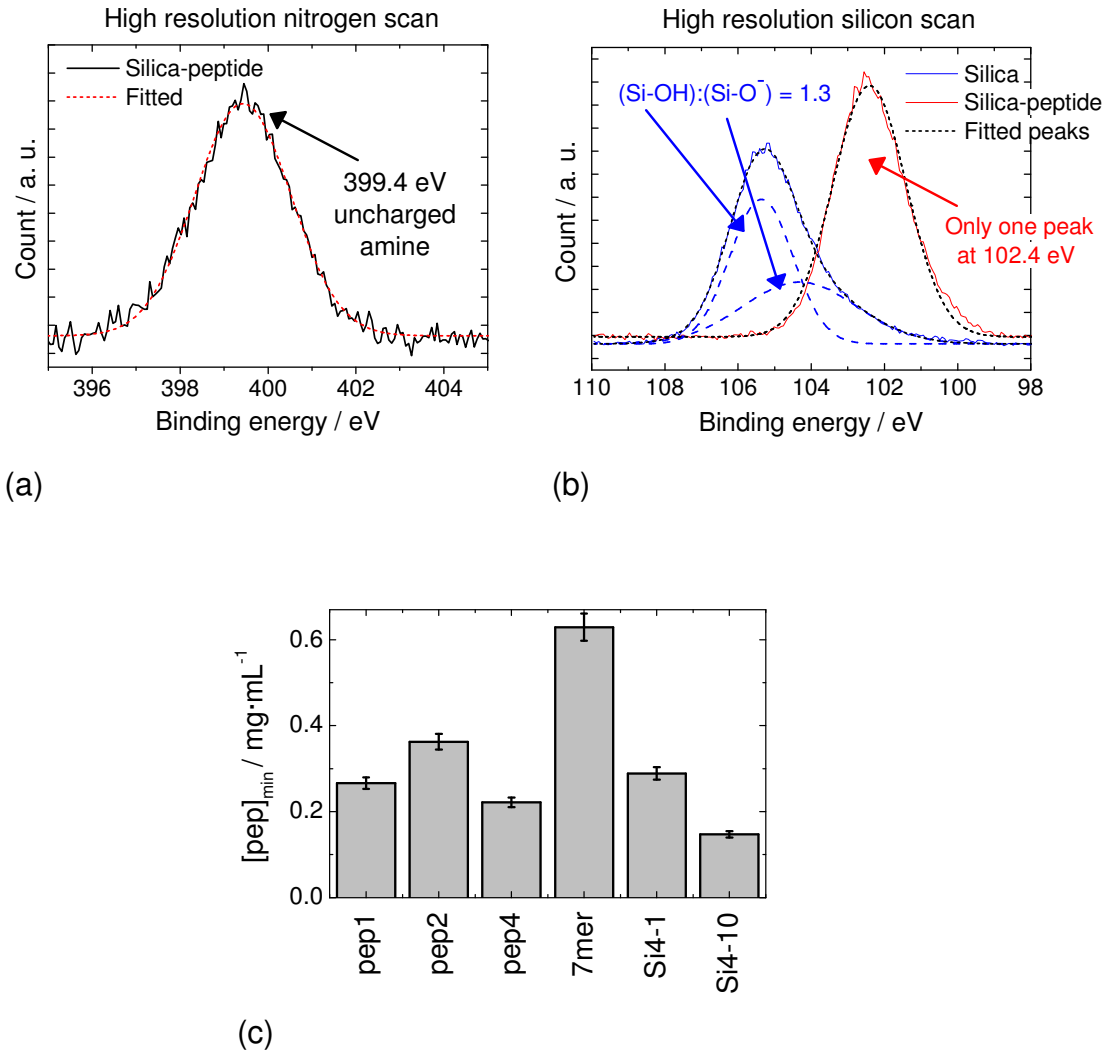

Figure S4. (a) High resolution XPS data for N 1s in dried silica-peptide samples. The N 1s peak indicates uncharged amine groups. (b) High resolution XPS data for Si 2p in silica-peptide samples vs silica. The Si 2p peak shifted significantly upon peptide adsorption. However, XPS could only be applied in the dry state and not under relevant solution conditions. (c) Minimum peptide concentration $[pep]_{min}$ required to attain ≥0.1 mg/mL adsorbed peptide on 82 nm silica particles.

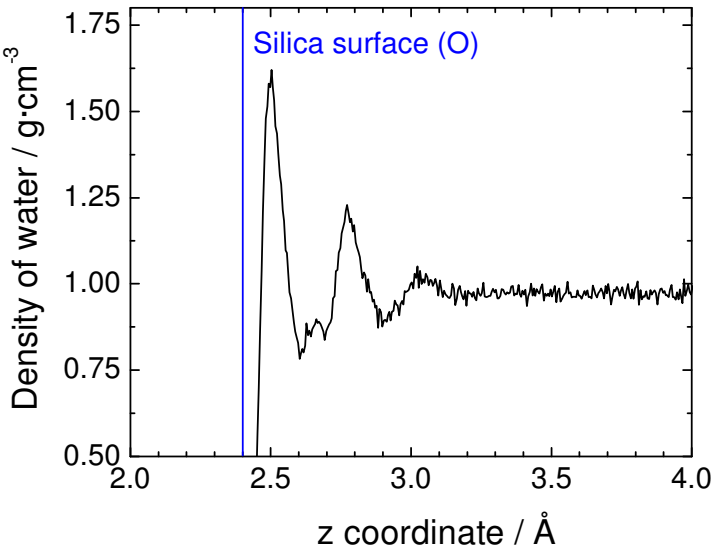

Figure S5. Computed density profile of water on a Q^3 silica surface with 50% ionization of silanol groups in the absence of peptide (average over 20 ns molecular dynamics simulation). The blue line represents the average position of superficial silanol oxygen atoms.

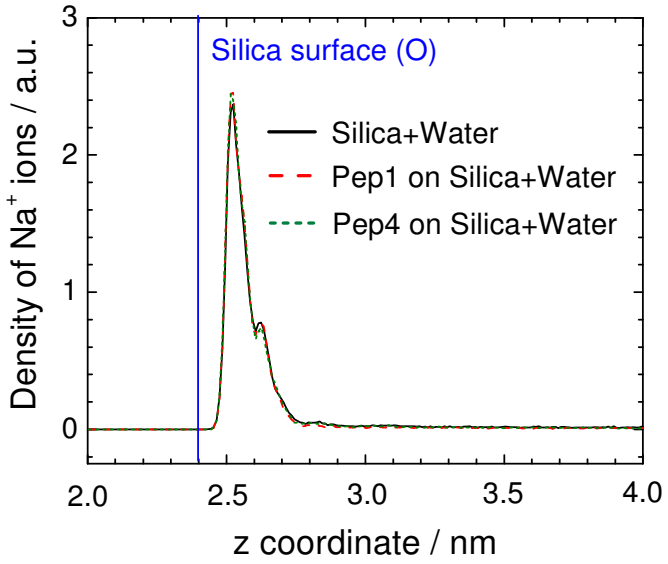

Figure S6. Computed density profile of Na^+ ions on a Q^3 silica surface with 50% ionization of silanol groups in the absence of peptides, in the presence of peptide pep1, and in the presence of peptide pep4 (average over 20 ns molecular dynamics simulation). The blue line represents the average position of superficial silanol oxygen atoms.

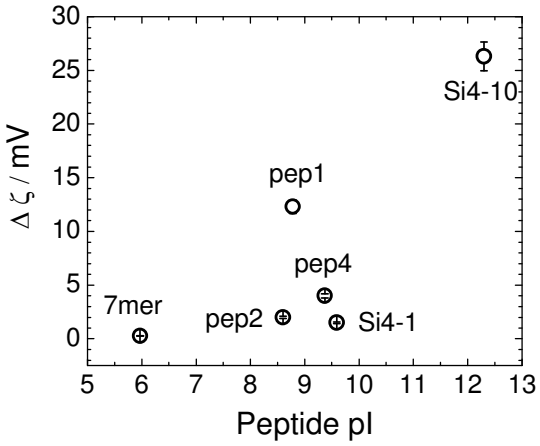

Figure S7. Change in zeta potential of 82 nm silica particles during an increase of peptide concentration from 0 to 1 mg mL^{-1} plotted as a function of peptide pI. A partial correlation with pI appears likely.

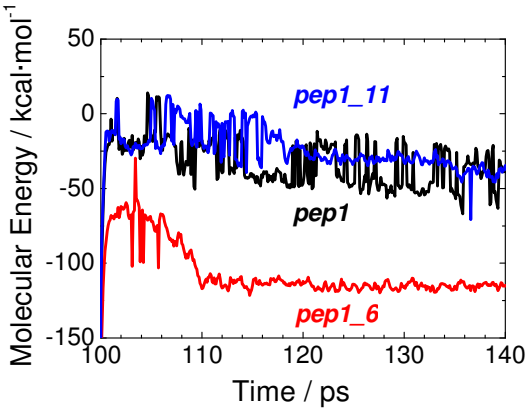

Figure S8. Total energy of the wild type pep1 sequence and of two variant sequences pep1_6 and pep1_11 in molecular dynamics simulation as a function of time. H-6 and H-11 were replaced by alanine, respectively, in pep1_6 and pep1_11.

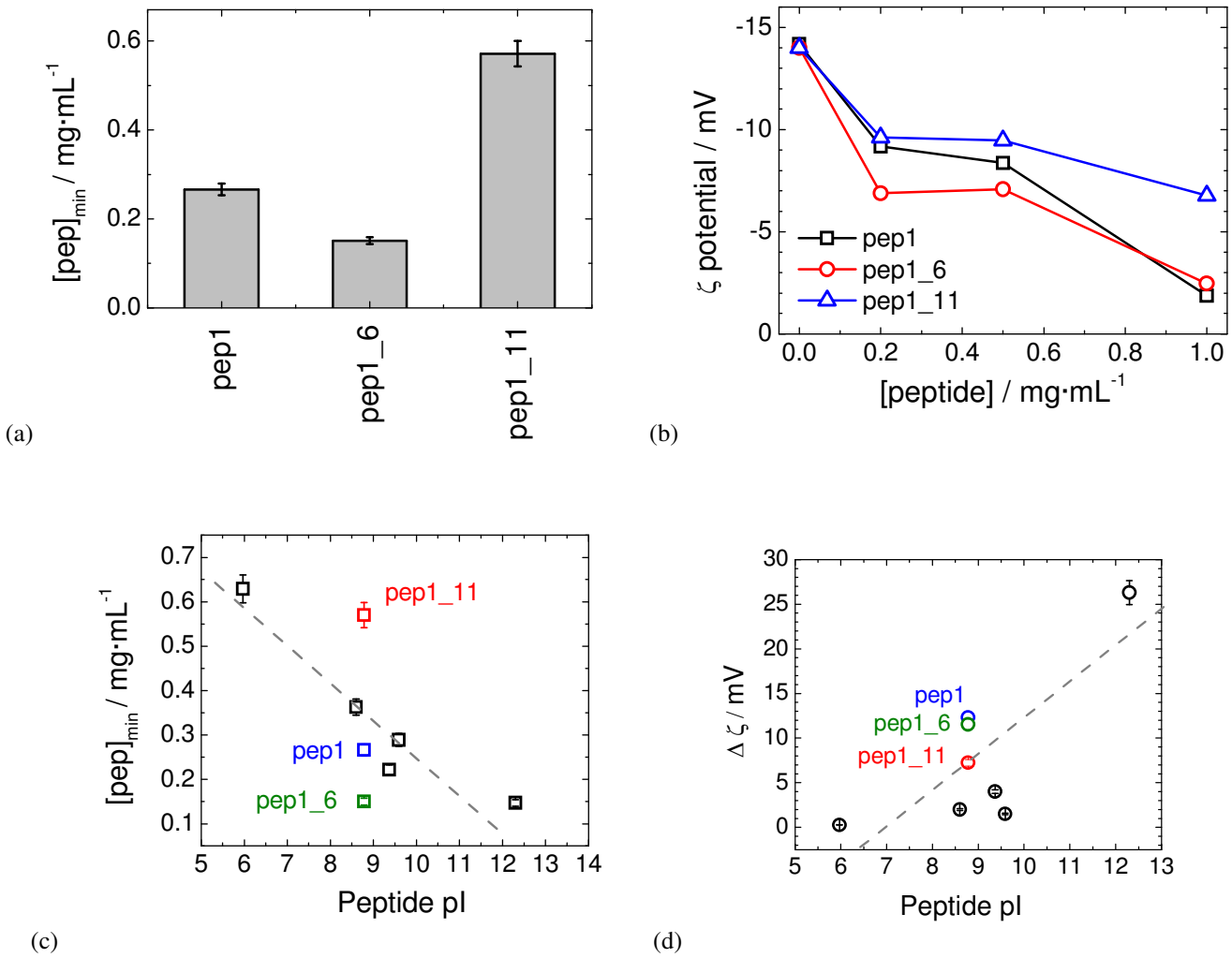

Figure S9. (a) Minimum initial concentration of pep1 and its mutants to achieve 0.1 mg/ml peptide binding to 82 nm silica particles. (b) Change in zeta potential of silica particles as a function of initial peptide concentration. (c) Minimum initial peptide concentration required to adsorb 0.1 mg/mL peptide. (d) Change in zeta potential of silica particles for an increase in initial peptide concentration from 0 to 1 mg mL^{-1}. For comparison, data for other peptides in Table 1 is also shown.

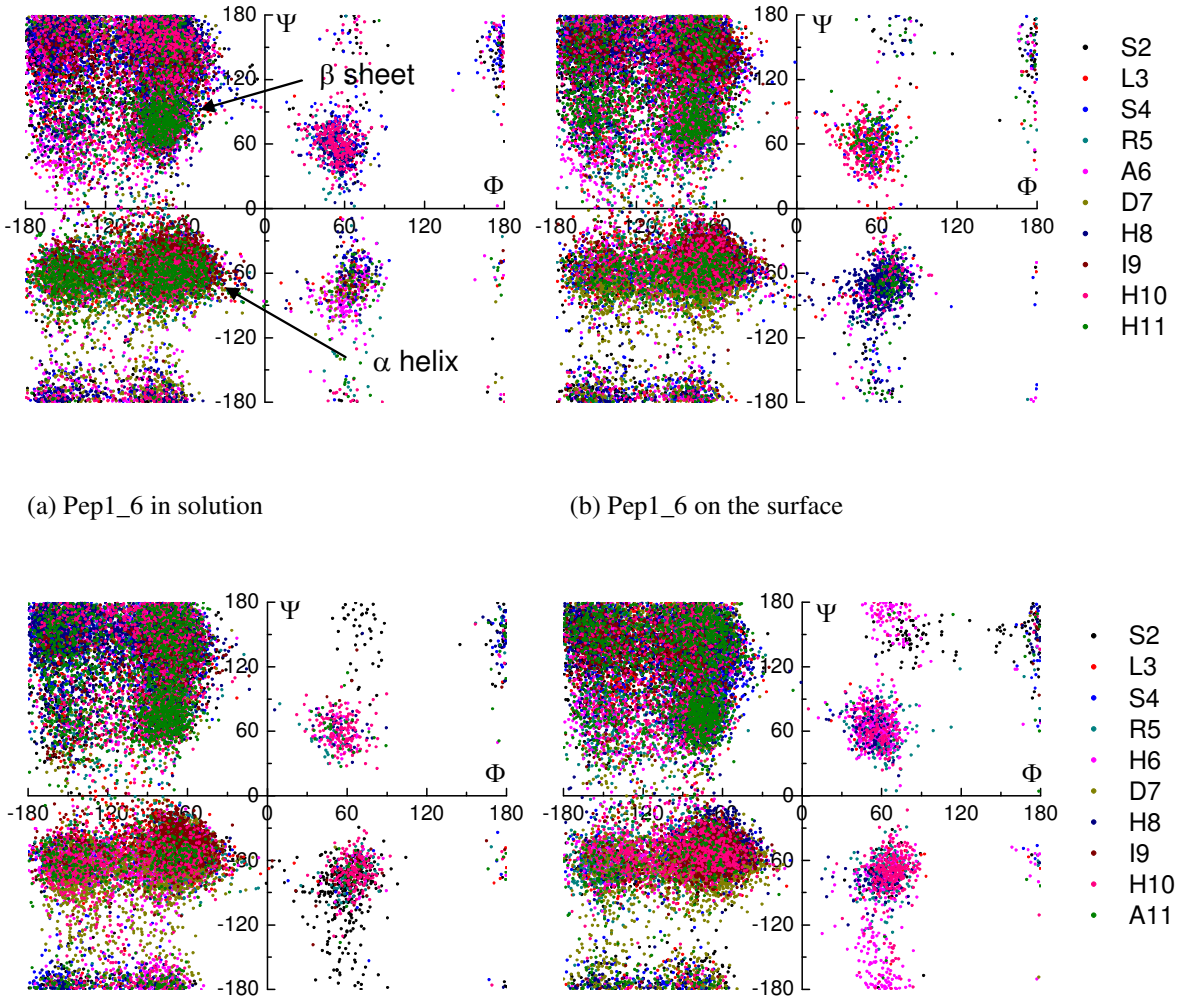

(a) Pep1_6 in solution

(b) Pep1_6 on the surface

(c) Pep1_11 in solution

(d) Pep1_11 on the surface

Figure S10. Ramachandran plots of (a) pep1_6 in solution, (b) pep1_6 on the Q^3 silica surface, (c) pep1_11 in solution, (d) pep1_11 on the Q^3 silica surface. Each plot contains 2000 data points per amino acid over a simulation time of 20 ns.

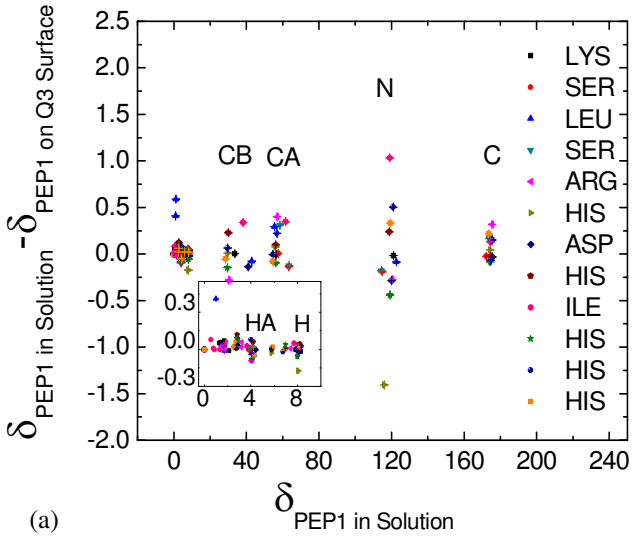
-δ PEP1 in Solution -δ PEP1 on Q3 Surface
δ PEP1 in Solution
CB CA
N
C
HA H
LYS
SER
LEU
SER
ARG
HIS
ASP
HIS
ILE
HIS
HIS
HIS

(a)

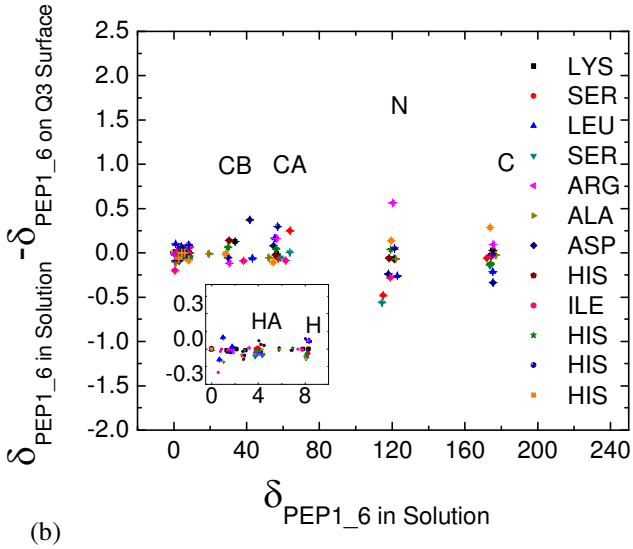
-δ PEP1_6 in Solution -δ PEP1_6 on Q3 Surface
δ PEP1_6 in Solution
CB CA
N
C
HA H
LYS
SER
LEU
SER
ARG
ALA
ASP
HIS
ILE
HIS
HIS
HIS

(b)

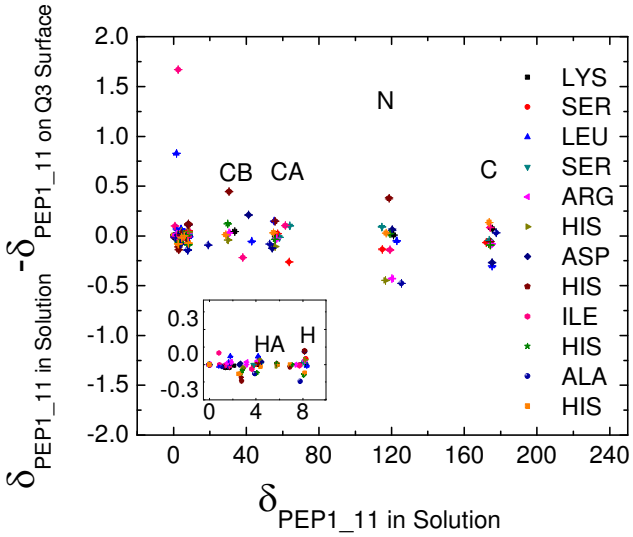
-δ PEP1_11 in Solution -δ PEP1_11 on Q3 Surface
δ PEP1_11 in Solution
CB CA
N
C
HA H
LYS
SER
LEU
SER
ARG
HIS
ASP
HIS
ILE
HIS
ALA
HIS

(c)

Figure S11. Change in computed ^{1}H, ^{13}C, and ^{15}N NMR chemical shifts of (a) pep1 (b) pep1_6 and (c) pep1_11 from solution state upon adsorption onto the Q^3 silica surface. Differences in chemical shifts are shown for the atoms CA, CB, N, C, HA, and H in each amino acid. Amino acids with significant changes in conformation exhibit larger differences. Every data point represents an average over 2000 snapshots over a simulation time of 20 ns.

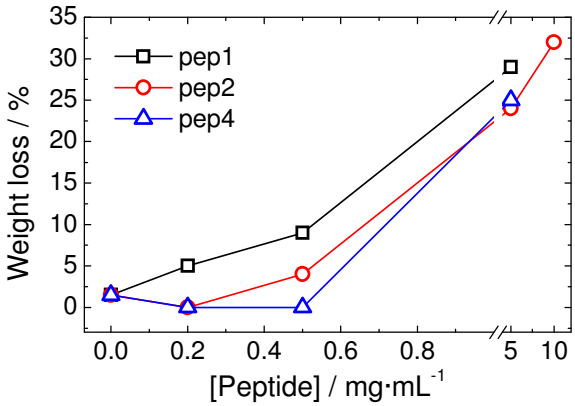

Figure S12. Weight loss calculated from TGA of silica particles prepared in the presence of various peptides as a function of initial peptide concentration.

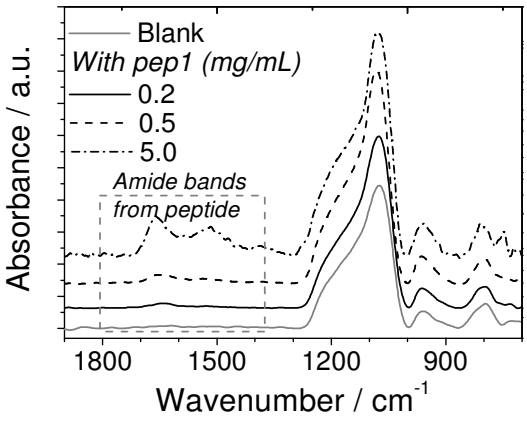

Figure S13. FTIR spectra of silica particles synthesised from SiCat in the presence of pep1 as a function of peptide concentration. The intense Si-O stretching vibration near 1000 cm^{-1} indicates the presence of silica, and the amide bands (highlighted) identify occluded peptide.

Additional References

(S1) (a) Kirschbaum, B. *Clin. Chim. Acta* **2001**, *308*, 147-153. (b) You, W. W.; Haugland, R. P.; Ryan, D. K.; Haugland, N. P. *Anal. Biochem.* **1997**, *244*, 277-282.

(S2) (a) Maple, J. R.; Thacher, T. S.; Dinur, U.; Hagler, A. T. *Chem. Des. Autom. News* **1990**, *5*, 5-10. (b) Sun, H.; Mumby, S. J.; Maple, J. R.; Hagler, A. T. *J. Am. Chem. Soc.* **1994**, *116*, 2978-2987. (c) Sun, H. *J. Comput. Chem.* **1994**, *15*, 752-768. (d) Hill, J.-R.; Sauer, J. *J. Phys. Chem.* **1994**, *98*, 1238-1244. (e) Sun, H. *Macromolecules* **1995**, *28*, 701-712.